JOURNAL OF AIRCRAFT
Vol. 38, No. 5, September–October 2001

Multipoint Aerodynamic Wing Optimization in Viscous Flow

J. Szmelter*
Cranfield University, Swindon, England SN6 8LA, United Kingdom

A methodology that allows for efficient aerodynamic optimization of wings with a full account of typical viscous effects is proposed. It extends earlier work by A. Jameson[1–3] on wing optimization for inviscid flows. The optimization process is based on control theory, which is employed to derive the adjoint equations. Accurate and consistent modeling of viscous effects is essential in wing design and is implemented in the approach described here by viscous-inviscid interaction. The solution involves interaction between the Euler solver and the two-dimensional boundary layer. Although this technique is limited by the known assumptions of the boundary-layer approximation, it is very well suited for civil aircraft wing design in cruise conditions. For applications where large viscous-dominated regions of separation are present, substantially more expensive design methods based on the Navier–Stokes equations have to be used. The method developed in this work has resulted in a practical engineering tool because it combines the benefits of the fast adjoint equation-based technique and a very economical boundary-layer approach. The cost required for viscous calculations is similar to that for inviscid flows. Results for three-dimensional wing design in viscous flow are possible, even with the use of a PC. The method is demonstrated for a single, clean wing, and wing-body configuration.

Nomenclature

A	=	wing surface area
Cd	=	drag coefficient calculated by pressure integration
C_e	=	entrainment coefficient
C_f	=	skin-friction coefficient
C_{f0}	=	skin-friction coefficient in equilibrium flow in zero pressure gradient
Cl	=	lift coefficient
Cp	=	pressure coefficient
C_τ	=	shear-stress coefficient
$H, \bar{H}, H_1$	=	velocity-profile shape parameters
M	=	Mach number
p	=	current pressure
pT	=	target pressure
U_e	=	mean component of streamwise velocity at edge of boundary layer
X, Y, Z	=	Cartesian coordinates
x	=	coordinate along surface
Θ	=	momentum thickness
λ	=	scaling factor on dissipation length

Subscripts

EQ	=	equilibrium conditions
EQ_0	=	equilibrium conditions in absence of secondary influences on turbulent structure

Introduction

AN important issue in aerodynamic design of transonic wings is to find the shape for minimum drag and/or maximum lift at given operating conditions. Over the years the traditional design has been aided by rapid developments in advanced numerical prediction and analysis methods, inverse design methods, and, more recently, optimization techniques. One of the critical elements of aerodynamic design has always been the high computational cost involved. The specific objective of the reported research has been to develop a truly efficient engineering tool, which would also allow for a representative modeling of flow physics.

The design technique presented in this paper is gradient-based and has been derived using control theory. It extends earlier work by A. Jameson[1–3] on wing optimization for inviscid flows. The control theory approach to optimal aerodynamic design, in which shape changes are based on gradient information, was first applied to transonic flows by Jameson.[4] The method originally formulated for inviscid compressible flows described by the potential equations has been further applied to the Euler equations[5] and the Navier–Stokes equations.[6] The method has been implemented for optimization of wings and wing-body configurations[3] as well as complex aircraft configurations.[7] In the context of aerodynamic optimization, the adjoint formulation has been adopted by many researchers, see, for example, Refs. 8–11. The approach is particularly attractive when aimed at specific applications and when computational speed and low memory requirements are needed. In the control theory sensitivity analysis the adjoint equations are derived and result in differential equations that are of the same order and character as the flow equations. Thus, the sensitivity with respect to an arbitrary number of design variables is obtained with the equivalent of only one additional flow calculation. In contrast to the traditional finite difference-based approach, the flow must be recalculated for perturbations in every design variable. Information about some other aerodynamic wing optimization methods can be found for example in Refs. 12 and 13 and literature provided therein.

For civil aircraft applications the accurate modeling of viscous effects poses an important class of problems. The work reported by Jameson et al.[6] describes wing optimization in viscous flow modeled by the Navier–Stokes equations. Although valuable, the method is still computationally expensive. An alternative, substantially cheaper approach is proposed, whereby the viscous-inviscid interaction method is used to account for viscous effects.

Flow solvers based on the viscous-inviscid interaction between full potential or Euler flow and boundary-layer codes are very well established for simple (i.e., wing alone or wing body) configurations. Indeed, the effectiveness of Euler codes has been significantly enhanced by the use of viscous coupled techniques. Today these single-block-topology-based suites of codes are extensively and routinely used by wing designers. Also, successful implementations of viscous-inviscid methods for complex aircraft configurations modeled by unstructured and multiblock-meshes-based methods have been demonstrated.[14] Viscous-inviscid interaction methods offer a valuable engineering tool suitable for specific classes of problems. The methods in general cannot be used for

Presented as Paper 99-0550 at the AIAA 37th Aerospace Sciences Meeting, Reno, NV, 11–14 January 1999; received 29 March 1999; accepted for publication 2 February 2001.

*Senior Lecturer, Department of Environmental and Ordnance Systems, Royal Military College of Science, Shrivenham; and Consultant, British Aerospace Airbus Limited.

the calculation of large, viscous-dominated regions of separation for which the Navier–Stokes equations have to be solved. When strong three-dimensional viscous effects are present, as for example is the case for highly swept wings, the use of three-dimensional boundary layers or Navier–Stokes solvers needs to be considered. However, with all of their well-known limitations viscous-inviscid interaction methods provide a valuable solution to many aerodynamic problems. In particular, those within the civil wing design process for which cruise drag reduction and buffet margins are critical make the ability to model transonic flow accurately essential.

By comparison with standard Navier–Stokes flow solvers, viscous-inviscid interaction methods are very efficient. The penalty for the incorporation of viscous effects does not, on average, exceed the order of 15% with respect to corresponding Euler solutions. The situation is even more cost advantageous when implemented in the wing optimization process. The proposed viscous-inviscid interaction method uses much larger elements than would be required by Navier–Stokes solvers and does not require the generation of highly stretched elements in the vicinity of the wall. By contrast, such elements are necessary for the solution of the Navier–Stokes equations. Consequently, for explicit flow solvers viscous-inviscid interaction methods allow much larger time steps to be used. Additionally, the modeling of turbulent flows achieved using the lag-entrainment boundary-layer approach is satisfactory for wing design applications and in practice is more accurate and consistent than standard turbulence models used in Navier–Stokes solvers.

For fast turnaround in the design process, the computing times required are very competitive and thus make the viscous-inviscid interaction techniques particularly suitable for implementation into inviscid flow optimization methods.

Design Procedure Considerations

Finding the best wing shape can be formulated by optimization. The solution of such an optimization is formulated for a transonic wing in viscous flow. The proposed design method is an extension of the work for inviscid flows, described in detail in Refs. 1–3. To derive the adjoint equations, control theory is applied directly to the Euler equations governing the inviscid flow solution. Therefore, in the adjoint equations solved here the effect of viscous terms is neglected. However, viscous terms are included in the flow solver as part of the design process via the Euler boundary-layer coupling. The gradient procedure is used as the optimization process. It follows the path of the steepest gradient to the local minimum.

The general design procedure, for a single design point, can be summarized by the following steps:

Step 1 Generate initial mesh

Step 2 Solve the coupled Euler/boundary-layer equations.

Step 3 Smooth the cost function if necessary, and set up boundary conditions for the adjoint equation.

Step 4 Update and solve the adjoint equations (viscous terms are neglected in the adjoint equation).

Step 5 Evaluate the gradient.

Step 6 Modify the profiles.

Step 7 Update the mesh to reflect the new shape.

Step 8 Return to Step 2 until general solution characteristics have been established.

In multipoint design steps 2–5 are performed for every design point separately, and the calculated gradients are weighted to provide combined global value used in step 6 to modify the shape.

During the optimization process, a single-block C-H topology mesh is generated for the wing using an analytical mesh generator with a square-root transformation. The changes of shape that are calculated in every design cycle are dependent on the mesh generator because these enter a definition of the transformation that requires updating. Hence, the physical locations of the mesh points are updated in the program for every design cycle. This is done in an inexpensive way, using exact analytical values from a mapping procedure. The adjoint equations when discretized are solved in a similar manner to the Euler part of the flow solution (for inviscid flows) to obtain the necessary gradient information. Once the gradient is calculated, a modification in shape can be made:

$$\text{modification in shape} = -\text{relaxation parameter} \times \text{gradient}$$

The modification in shape is measured in terms of the wing thickness defined in a transformed plane. To make sure that the redesigned shape remains smooth, the shape change is smoothed by both explicit and implicit procedures. In the method the shape change ensures a reduction in a cost function. After making such a modification, the gradient can be recalculated, and the process is repeated until a minimum is reached. There is a possibility of more than one local minimum, but in any case the method should lead in the direction of an optimized shape.

The optimization implemented in the code can be used to provide drag reduction or inverse design capability.

Currently the following cost function is available:

$$\text{Cost function} = 0.5\ \text{weight}\ 1 \int (p - pT)\,\mathrm{d}A + \text{weight}\ 2\, Cd + 0.5\ \text{weight}\ 3 \int (\mathrm{d}p/\mathrm{d}X)\,\mathrm{d}A \tag{1}$$

where an initially guessed target pressure pT is updated during solution. When in expression (1) only the difference between current and target pressure is used

$$\text{Cost function} = 0.5 \int (p - pT)\,\mathrm{d}A \tag{2}$$

the optimization process can be viewed as an inverse design.

Because the inverse design concept is realized in the form of an optimization procedure, the procedure should still provide some solution for problems for which it is difficult to formulate desired aerodynamic targets and geometric constraints, e.g., three-dimensional problems and for which a classical inverse design method would be limited in its application.

Flow Equations and Solution

A viscous flow model is based on the viscous inviscid interaction. It employs semi-inverse coupling between the Euler solver and the two-dimensional integral boundary-layer method. For typical civil aircraft wings, in cruise condition, three-dimensional viscous effects are strong only in the close vicinity of a wing tip. Therefore, the use of a two-dimensional boundary layer is in this case adequate. For highly swept military aircraft wings three-dimensional boundary layers or Navier–Stokes solvers should be used. The Euler solver is based on the Runge–Kutta multistage time-stepping scheme. The basic space discretization is accomplished by employing a finite volume, cell-centered scheme of Jameson.[15–17] The flow solver has implicit residual smoothing and local time-stepping capabilities. The semi-inverse viscous-inviscid interaction technique of Le Balleur[18] has been introduced to improve stability in flows close to separation. The integral laminar/turbulent boundary-layer method, pioneered at Defence Evaluation and Research Agency (DERA), uses either a prescribed pressure distribution (direct mode) or the predicted growth in displacement thickness (inverse mode) to drive the boundary-layer equations (Fig. 1). The approach is based on the lag-entrainment method,[19,20] which has been further developed by DERA to incorporate curvature effects on turbulence structure,[21] compressibility effects,[22] low-Reynolds-number correction, normal shear-stress terms as well as wake calculation.[23] For completeness the summary of the lag-entrainment method is provided:

Continuity:

$$\frac{\Theta\,\mathrm{d}\bar{H}}{\mathrm{d}x} = \frac{\bar{\mathrm{d}}H}{\mathrm{d}H_1}\left\{C_c - H_l\left[\frac{C_f}{2} - (H+1)\frac{\Theta}{U_c}\frac{\mathrm{d}U_c}{\mathrm{d}x}\right]\right\} \tag{3}$$

Momentum:

$$\frac{\mathrm{d}\Theta}{\mathrm{d}x} = \frac{C_f}{2} - (H + 2 - M^2)\frac{\Theta}{U_c}\frac{\mathrm{d}U_c}{\mathrm{d}x} \tag{4}$$

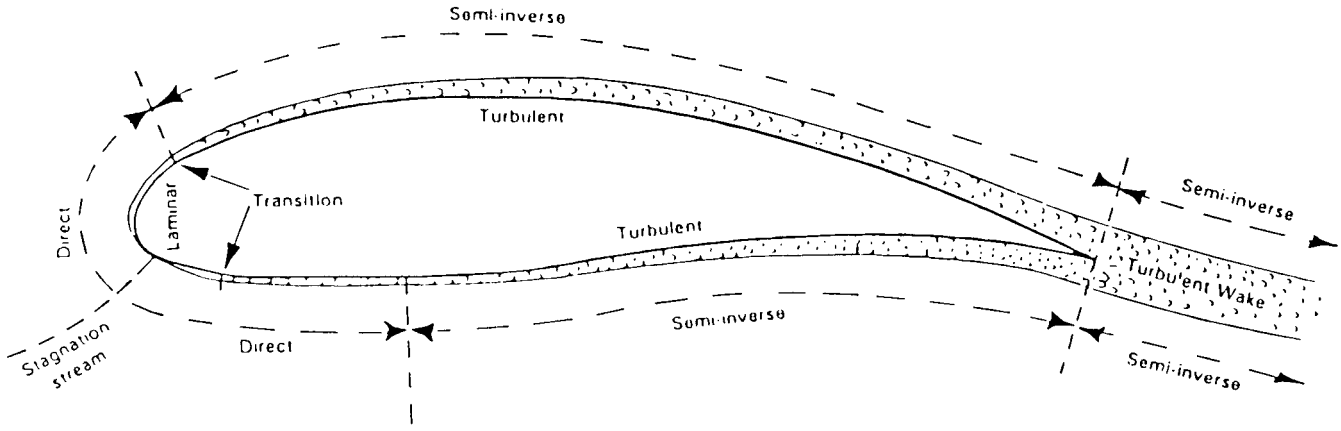

Fig. 1 Euler boundary-layer coupling.

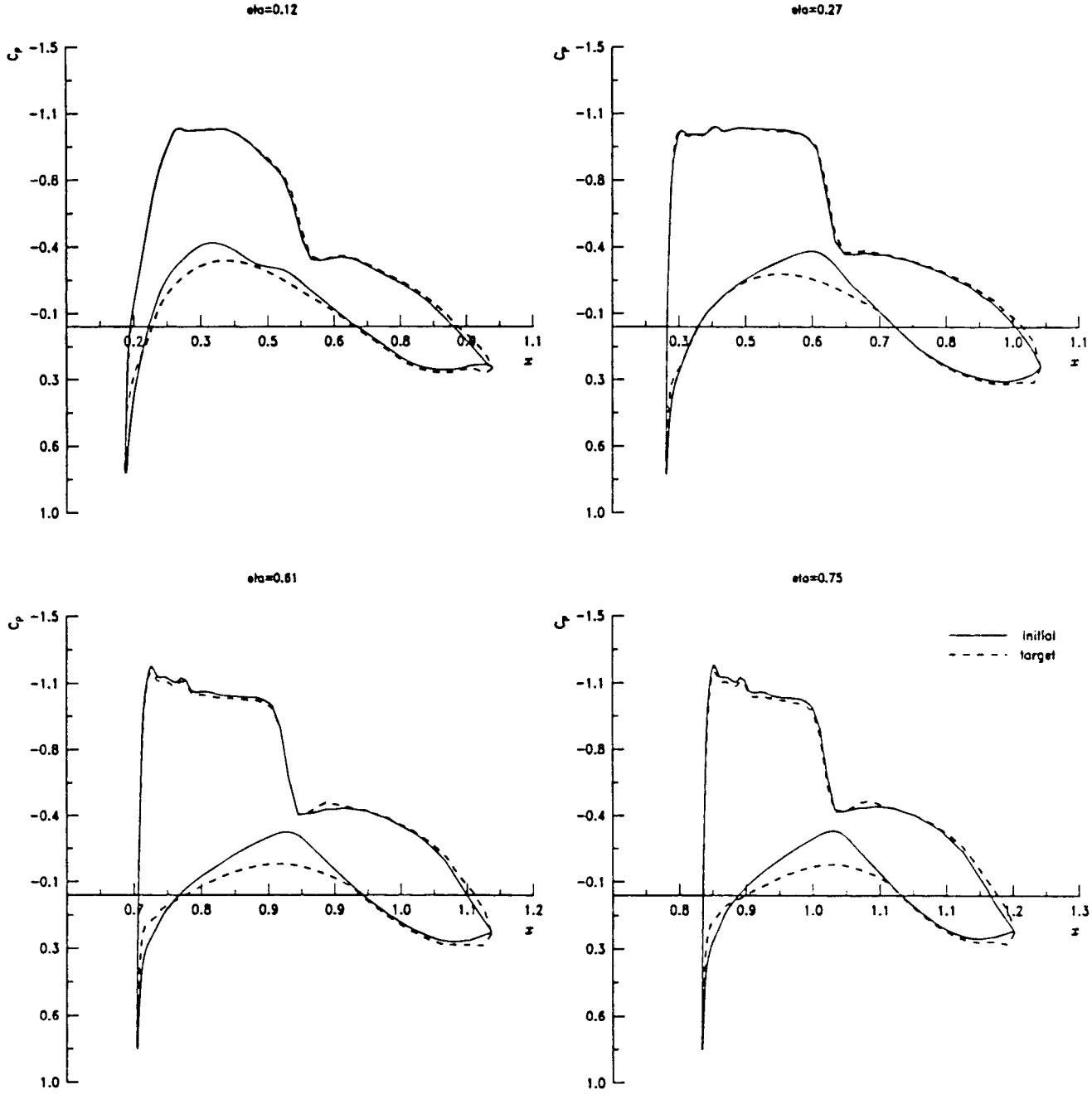

Fig. 2 Comparison of initial and target pressures.

Lag-entrainment:

$$\frac{\Theta\, dC_c}{dx} = F\left\{\frac{2.8}{H+H_1}\left[(C\tau)^{0.5}_{EQ_0} - \lambda C_\tau^{0.5}\right] + \left(\frac{\Theta}{U_c}\frac{dU_c}{dx}\right)_{EQ}\right.$$

$$\left. - \frac{\Theta}{U_c}\frac{dU_c}{dx}\left[1 + 0.075M^2\frac{(1+0.2M^2)}{(1+0.1M^2)}\right]\right\} \quad (5)$$

where F is the function of C_e and C_f.

$$F = \frac{\left(0.02C_c + C_c^2 + 0.8C_{f0}/3\right)}{(0.01 + C_c)} \quad (6)$$

The laminar portion of the boundary layer is calculated by the Thwaites compressible method, with transition predicted by the Granville correlation criterion. With forced transition the laminar separation bubble is calculated by Horton's method.

For applications to realistic civil aircraft configurations, it is important that the theoretical design/prediction tools are not only able to calculate well-behaved attached laminar and turbulent flows, but also to handle off-design behavior such as shock-induced and trailing-edge boundary-layer separation and the interaction between shock-induced and trailing-edge separation. This capability was demonstrated first by DERA.[24] Le Balleur has extended the semi-inverse coupling method to deal with massively separated flows.[25]

Adjoint Equations

The adjoint equations solved here are identical to those derived for inviscid flow in Ref. 3, where control theory has been applied to the Euler equations. At this stage of development, viscous effects in the adjoint equations are omitted. The consequences of this omission need to be further investigated. Nevertheless, it is likely that in cruise conditions, which are of the primary interest here and for which viscous coupling techniques are particularly suitable, the influence

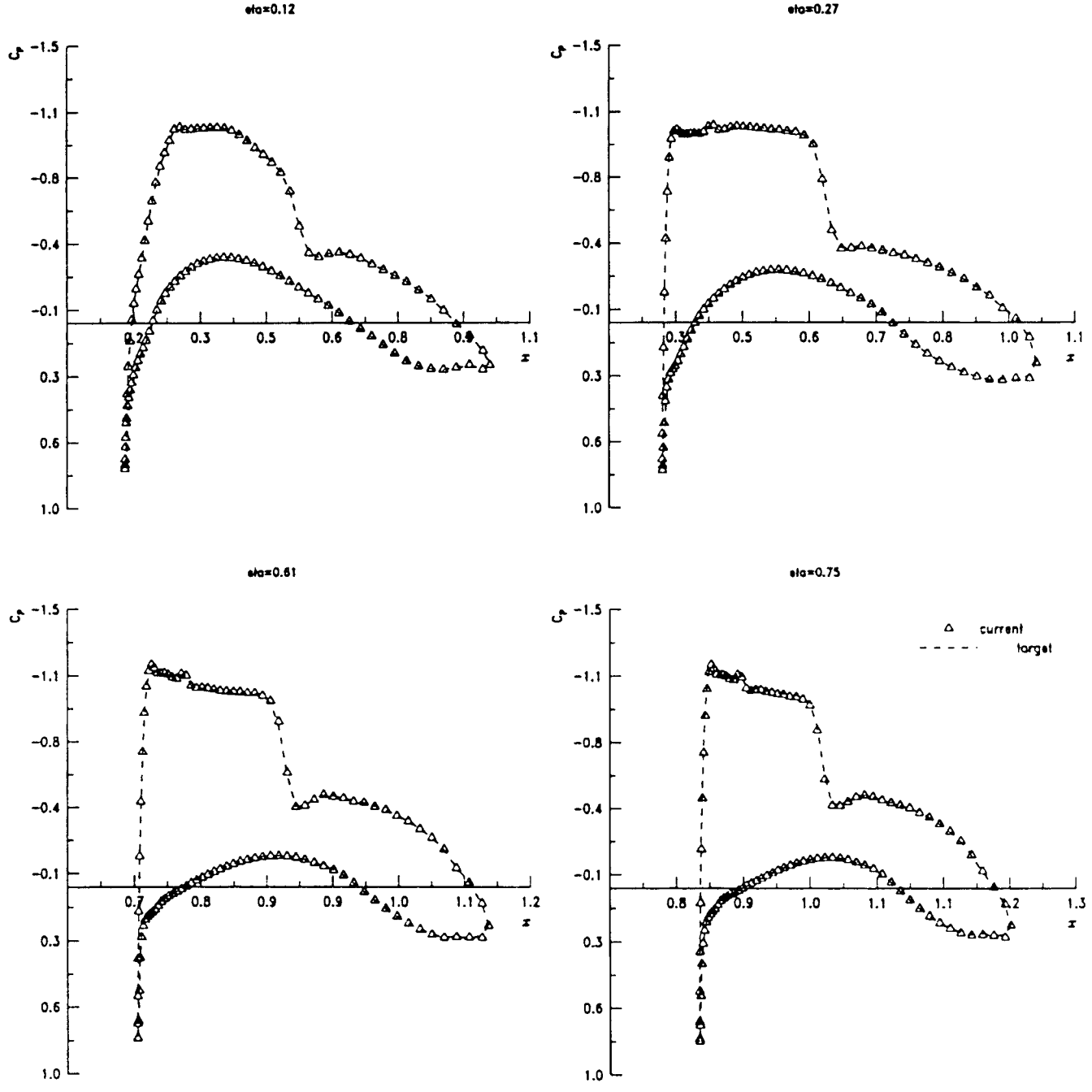

Fig. 3 Comparison of current and target pressures.

of viscous terms in the adjoint equations is minor. Some additional insight in the context of the Navier–Stokes equations can be found in Ref. 4.

The solution of the adjoint equations is similar to the Euler part of the flow solution. The fluxes are first estimated by central differences and then modified by downwind biasing through numerical diffusive terms. These are supplied by similar subroutines to those used for the inviscid flow solution.

Numerical Results

To provide at least some illustration of the proposed method, one example of inverse design problem, which confirm the validity of the method, and one example of a drag reduction have been selected.

Apart from the standard validation of the code run as a flow solver only, it is worth mentioning that a simple control test case provided a valuable example for the initial validation of the code. Namely, an inverse design run has been performed, which prescribed a target pressure identical to the current pressure obtained by the flow solver on the initial geometry. Correctly the code "did nothing," i.e., the wing geometry remained unchanged. Close examination has shown a difference of the order of fifth decimal figure. This is caused by interpolation procedures, which, even in such straightforward case, are performed automatically by the program.

For the single-wing case presented here a W4 wing geometry[26] has been used. Because this geometry is provided in a wing/body configuration, the wing has been modified by the introduction of an additional extended root section in order to create a representative single wing geometry. All test cases have been performed using $160 \times 32 \times 32$ size mesh. Only values for the pressure drag are quoted.

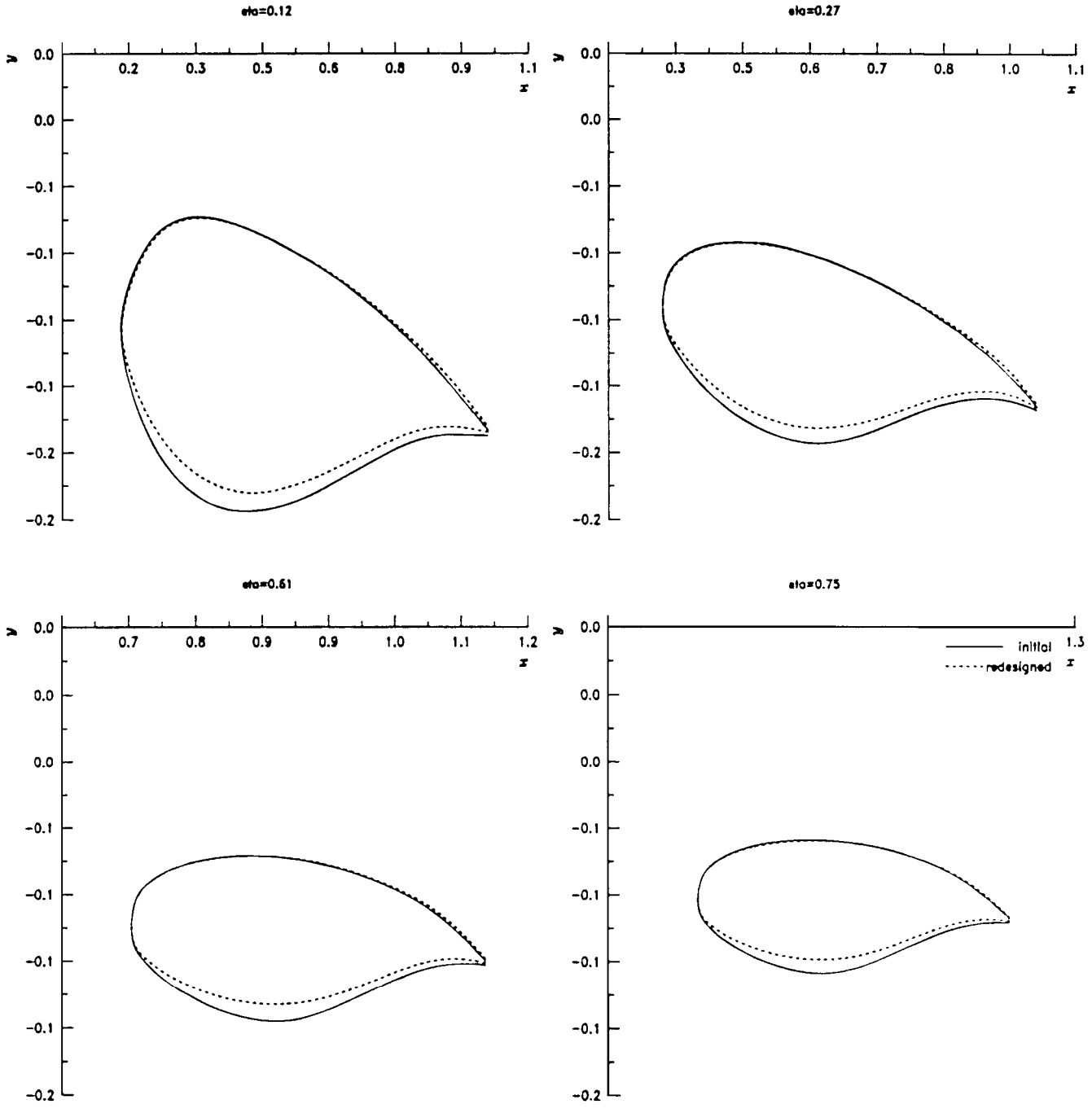

Fig. 4 Comparison of initial and redesigned geometries.

Test Case 1 Modifications in Region of Wing Box—W4 at $M = 0.78$, $\alpha = 0.52$, and $Re = 8.5 \times 10^6$

This test case is aimed at investigating the capability of the inverse design option of the code to redesign the wing to gain extra lift (hence lift over drag L/D) by prescribing an increase in the lower surface-pressure levels in the region of the wing box, between $20\% < X/c < 60\%$ at specified span stations. The geometrical constraints desired in such an exercise to retain twist and maximum aerofoil thickness with respect to local chord (t/c max.) have not been applied. The pressure coefficient Cp distribution obtained by the initial flow solution was modified to generate a new lower surface target pressure in the region of the wing box to increase the lift coefficient Cl. This target pressure was used to perform 40 inverse design cycles. The results at four selected sections are given in Figs. 2–5. In Fig. 2 the initial pressure coefficient Cp distribution for W4 wing is compared with the prescribed Cp target. In Fig. 3 Cp target distribution and Cp distribution from the solution obtained on the redesigned geometry after 40 cycles are compared and show close match for all sections. The corresponding redesigned sections are compared

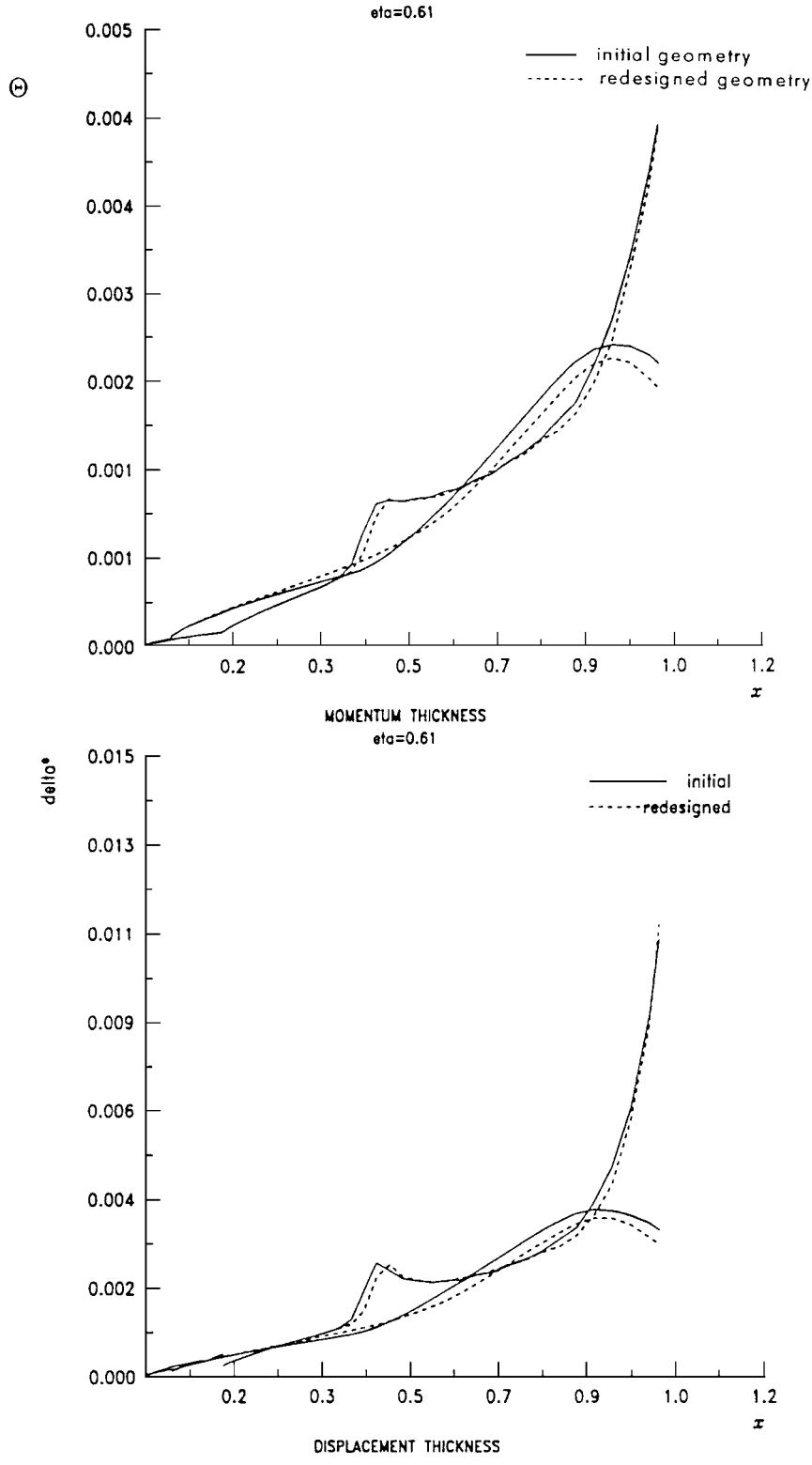

Fig. 5 Boundary-layer parameters.

with the initial geometry in Fig. 4. Relative to the target pressure distribution, only minor changes or no change at all occurred on the upper surface. The final $Cl = 0.5701$ increased relative to the initial solution $Cl = 0.5265$, pressure drag $Cd = 0.0198$ increased from the initial $Cd = 0.0191$. The final angle of attack is $\alpha = 0.4706$. In this inverse design exercise the overall target pressure was achieved at the expense of a thinner wing.

Investigation of a history of a design indicated that little improvement is made after the 10th cycle, while the Cp in the trailing-edge region slightly deteriorates. The modifications to the lower surface change the aerofoils into thinner sections. The largest changes occur in the first 10 design cycles, approaching convergence approximately in 10 cycles when little change is made. Some improvement in performance can usually be obtained by better calibration of smoothing and relaxation parameters used by the code. An example of the representative change in the momentum and displacement thickness is illustrated in Fig. 5 for one selected section at $\eta = 0.61$, where the initial and optimized designs are shown. The position of the shock did not change during the optimization. The effect the shock has on the displacement and momentum thickness is clearly visible at about 4.5 local chord and corresponds to the shock position indicated in Cp plots in Fig. 2 (scaled to a wing's root chord). In this example the code was run with transition fixed at 0.15 and 0.05 local chord for the upper and lower surfaces respectively; this is reflected in the boundary-layer parameters shown in Fig. 5. A transition point for the upper surface of the initial geometry manifests itself particularly clearly in the displacement thickness plot by a discontinuity in the solid line. CPU required for 40 design cycles is 17,000 s on CRAY J90 and is representative of most calculations. Interestingly, the comparison with CPU time required by

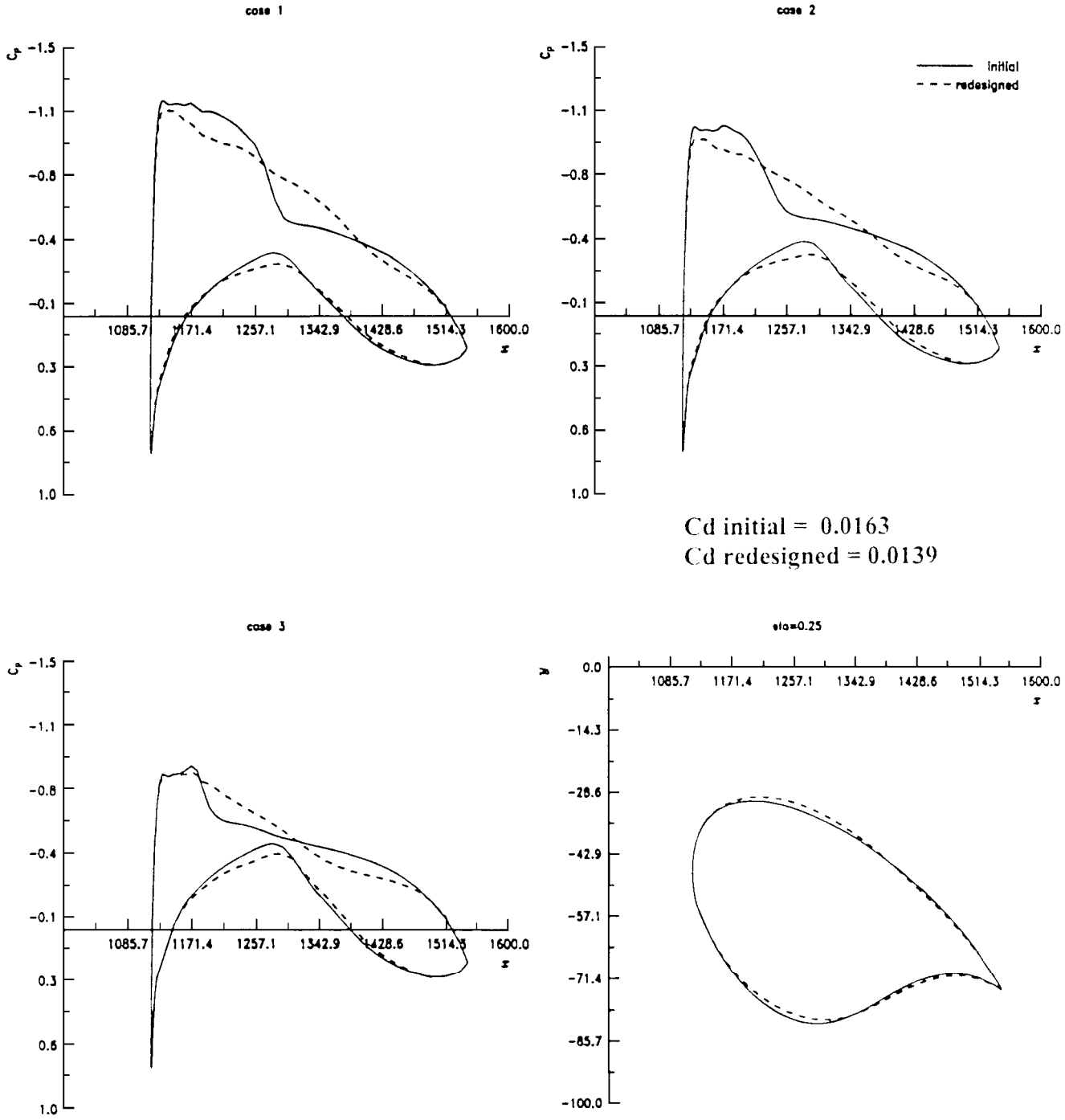

Fig. 6 Comparison of initial and current pressures and geometry after multipoint optimization.

Table 1

Design point	α	Cl	Cd	Weight
1	1.52	0.6490	0.0249	1
2	0.52	0.5084	0.0163	2
3	−0.48	0.3834	0.0091	1

the inviscid code to achieve similar targets shows that the viscous code is slightly faster even despite disabled multigrid capabilities. If confirmed by further investigations, this can indicate a stabilizing effect of boundary layer on the design process.

Test Case 2 Multipoint Drag Reduction Optimization

The three-point drag optimization option was tested for the wing W4 wing body configuration defined in Ref. 24 (but the geometry of the fuselage has been modified to be more realistic than a indefinite axysymmetric body). First the flow solution was obtained at mach number $M = 0.78$, $Re = 8.5 \times 10^6$ and lref $= 0.91$. Table 1 shows that for the following three angles of attack α the corresponding values of Cl and Cd were obtained.

Next, 40 design cycles were run. The initial target pressure was taken from the flow solution obtained for the initial wing body geometry and was smoothed. During the design process, the pressure was reset every four cycles and again smoothed. The Cl target was prescribed for every design point to the values just quoted. As indicated by the weights, the second design point was mainly targeted. The solution obtained for the modified shape showed that for the first and third design points the Cd and α were not substantially different from the initial values. For the design point Cd decreased to 0.0139, and the final α was 0.04746. In this sample run very conservative parameters were chosen so that only small changes in design were allowed.

In Fig. 6 the initial and current pressures are compared for a selected section at $\eta = 0.25$ and illustrate the tendency of the method to smooth the shock. A change in shape for this section is also shown.

Conclusions

A practical method for three-dimensional wing optimization in viscous flows is presented. The performance of the method has been illustrated for single wing examples and shows that viscous effects can be adequately modeled. The method requires modest CPU time, and more speed can be achieved by implementation of multigrid and parallelization of the code.

Despite producing good engineering results, the method needs to be further studied. In particular, the consequences of omitting viscous terms in the solution of the adjoint equations, in combination with the boundary-layer assumptions, should be better understood.

The concept of using viscous-coupling techniques in control-theory-based optimization methods is general and can be extended to codes that are currently capable of optimizing complex geometries in inviscid flows.

Acknowledgments

This research was carried out under Contract to British Aerospace Airbus Limited. All rights reserved (c) Copyright 1998, BRITISH AEROSPACE PLC with whose permission this paper is reproduced. The author is particularly grateful to A. Jameson for his help.

References

[1]Jameson, A., "Optimum Aerodynamic Design via Boundary Control," AGARD FDP/Von Karman Inst. Lecture Notes on Optimum Design Methods in Aerodynamics, AGARD Rept. 803, Brussels, April 1994, pp. 3-1–3-33.

[2]Jameson, A., "Optimum Aerodynamic Design Using CFD and Control Theory," AIAA Paper 95-1729, June 1995.

[3]Reuther, J., and Jameson, A., "Aerodynamic Shape Optimisation of Wing and Wing-Body Configurations Using Control Theory," AIAA Paper 95-0123, Jan. 1995.

[4]Jameson, A., "Aerodynamic Design via Control Theory," *Journal of Scientific Computing*, Vol. 3, 1988, pp. 233–260.

[5]Jameson, A., and Reuther, J., "Control Theory Based Airfoil Design Using the Euler Equations," AIAA Paper 94-4272, Jan. 1994.

[6]Jameson, A., Pierce, N., and Martinelli, L., "Optimum Aerodynamic Design Using the Navier–Stokes Equations," AIAA Paper 97-0101, Jan. 1997.

[7]Reuther, J., Jameson, A., Farmer, J., Martinelli, L., and Saunders, D., "Aerodynamic Shape Optimisation of Complex Aircraft Configurations via an Adjoint Formulation," AIAA Paper 96-0094, Jan. 1996.

[8]Burgreen, G. W., and Baysal, O., "Three-Dimensional Aerodynamic Shape Optimisation of Wings Using Sensitivity Analysis," AIAA Paper 94-0094, Jan. 1994.

[9]Gallman, J., Reuther, J., Pfeiffer, N., Forrest, W., and Bernstorf, D., "Business Jet Wing Design Using Aerodynamic Shape Optimisation," AIAA Paper 96-0554, Jan. 1996.

[10]Pironneau, O., "Optimal Shape Design for Aerodynamics," AGARD FDP/Von Karman Inst., Lecture Notes on Optimum Design Methods in Aerodynamics, AGARD Rept. 803, Brussels, April 1994, pp. 6-1–6-40.

[11]Baysal, O., and Eleshaky, M. E., "Aerodynamic Design Optimisation Using Sensitivity Analysis and Computational Fluid Dynamics," *AIAA Journal*, Vol. 30, No. 3, 1992, pp. 718–725.

[12]AGARD FDP-Von Karman Inst. for Fluid Dynamics, Lecture Notes on Optimum Design Methods in Aerodynamics, Brussels, April 1994.

[13]Foster, N. F., and Dulikravich, G. S., "Three-Dimensional Aerodynamic Shape Optimisation Using Genetic Evolution and Gradient Search," AIAA Paper 96-0555, Jan. 1996.

[14]Szmelter, J., "Viscous Coupling Techniques Using Unstructured and Multiblock Meshes," *Proceedings of 20th International Council of the Aeronautical Sciences Conference*, ICAS-96-1.7.4, 1996, pp. 1457–1467.

[15]Jameson, A., "Solution of the Euler Equations by a Multigrid Method," *Applied Mathematics and Computation*, Vol. 13, 1983, pp. 327–356.

[16]Jameson, A., "Transonic Flow Calculation for Aircraft," *Numerical Methods in Fluid Dynamics*, edited by F. Brezzi, Lecture Notes in Mathematics, Vol. 1127, Springer-Verlag, 1985, pp. 156–242.

[17]Jameson, A., "Multigrid Algorithms for Compressible Flow Calculations," *Proceedings of the Second European Conference on Multigrid Methods*, edited by U. Trottenberg et al., Lecture Notes in Mathematics, Vol. 1228, Springer-Verlag, 1986, pp. 166–201.

[18]Le Balleur, J. C., "Calcul par Copulage Fort des Ecoluements Visqueux Trannssoniquues Incluant Sillages et Decollemants. Profils d'Aile Portant," La Recherche Aerospatiale, No. 3, 1981, pp. 161–185.

[19]Green, J. E., Weeks, D. J., and Brooman, J. W. F., "Prediction of Turbulent Boundary Layers and Wakes in Compressible Flow," Royal Aircraft Establishment, Technical Rept. TR-2231, UK, 1973.

[20]Green, J. E., "Application of Head's Entrainment Method to the Prediction of Turbulent Boundary Layers and Wakes in Compressible Flow," Royal Aircraft Establishment, Technical Rept. TR72079, UK, 1972.

[21]Bradshaw, P., "The Analogy Between Streamline Curvature and Buoyancy in Turbulent Shear Flow," *Journal of Fluid Mechanics*, Vol. 31, Pt. 4, 1968, pp. 753–778.

[22]Green, J. E., "The Prediction of Turbulent Boundary Layer Development in Compressible Flow," *Journal of Fluid Mechanics*, Vol. 31, Pt. 4, 1968, pp. 753–778.

[23]Squire, H. B., and Young, A. D., "The Calculation of the Profile Drag of Aerofoils," Aeronautical Research Council, R&M, 1838, UK, 1937.

[24]Williams, B. R., "The Prediction of Separated Flows Using a Viscous-Inviscid Interaction Method," Royal Aircraft Establishment, TM Aero 2010, UK, 1984.

[25]Le Balleur, J. C., "Vicsous-Inviscid Calculation on High Lift Separated Compressible Flow over Airfoils and Wings," *Proceedings*, AGARD CP-515, Banff, Oct. 1992.

[26]Fulker, J. L., "Pressure Distributions on Research Wing W4 Mounted on an Axisymmetric Body, Case B3," *A Selection of Experimental Test Cases for the Validation of CFD Codes*, Vols. 1 and 2, AGARD-AR-303, 1994.